

**Detection of a new methanol maser line with the Kitt Peak 12–m  
telescope by remote observing from Moscow.**

V.I. Slysh<sup>1</sup>, S.V. Kalenskii<sup>1</sup>, I.E. Val'tts<sup>1</sup> and V.V. Golubev<sup>2</sup>

Received \_\_\_\_\_; accepted \_\_\_\_\_

arXiv:astro-ph/9701075v1 14 Jan 1997

---

<sup>1</sup>Astro Space Center, Lebedev Physical Institute, Profsoyuznaya str. 84/32, 117810, Moscow, Russia; vslysh@dpc.asc.rssi.ru; kalensky@socrat.asc.rssi.ru; ivaltts@dpc.asc.rssi.ru.

<sup>2</sup>Astronomical Division, Moscow State University, Vorob'evy Gory, 119899, Moscow, Russia; golubev@dpc.asc.rssi.ru.

## ABSTRACT

A new methanol maser line  $6_{-1} - 5_0 E$  at 133 GHz was detected with the 12-m Kitt Peak radio telescope using remote observation mode from Moscow. Moderately strong, narrow maser lines were found in DR21(OH), DR21-W, OMC-2, M8E, NGC2264, L379, W33-Met. The masers have similar spectral features in other transitions of methanol- $E$  at 36 and 84 GHz, and in transitions of methanol- $A$  at 44 and 95 GHz. All these are Class I transitions, and the new masers also belong to Class I. In two other methanol transitions near 133 GHz,  $5_{-2} - 6_{-1} E$  and  $6_2 - 7_1 A^+$ , only thermal emission was detected in some sources. Several other sources with wider lines in the transition  $6_{-1} - 5_0 E$  also may be masers, since they do not show any emission at the two other methanol transitions near 133 GHz. These are NGC2071, S231, S255, GGD27, also known as Class I masers. The ratio of intensities and line widths of the 133 GHz masers and 44 GHz masers is consistent with the saturated maser model, in which the line rebroadening with respect to unsaturated masers is suppressed by cross relaxation due to elastic collisions.

*Subject headings:* ISM : molecules — masers — radio lines: ISM

## 1. Introduction

The widespread galactic methanol masers were found in many transitions in the microwave band. Two kinds of sites are associated with methanol masers. Cold dust cores sometimes containing star formation regions at a very early, pre-stellar stage of evolution are associated with Class I methanol masers. They emit in a particular set of methanol transitions at 25, 36, 44, 84, and 95 GHz. Another kind of star formation regions with young stars which are embedded in nascent molecular cores and produce ultra-compact HII regions, is associated with methanol masers of Class II. They emit lines in a different from Class I set of transitions, typically, at frequencies 6.7 and 12 GHz. Recently a new Class II methanol maser line was detected at a very high frequency 157 GHz (Slysh et al. 1995) (see Menten (1991) for an earlier discussion of methanol maser classification). Masers of Class I in methanol- $E$  were found in transitions between the levels of the  $K = -1$  stack and those of the  $K = 0$  stack. Zuckerman et al. (1972) proposed a model of maser inversion by collisional excitation of molecules, followed by radiative decay. A much faster spontaneous decay of the  $K = 0$  levels leads to their underpopulation relative to the  $K = -1$  levels, which results in the inversion of the transitions between the  $K = -1$  and  $K = 0$  levels. Masers are expected in transitions  $J_{-1} - (J - 1)_0 E$  with  $J \geq 4$ , when the  $J_{-1}$  levels become higher than the  $(J - 1)_0$  levels. The first transition of this type is  $4_{-1} - 3_0 E$ , at 36 GHz, and was discovered as a maser by Morimoto et al. (1985) in Sgr B2. The second transition,  $5_{-1} - 4_0 E$ , was discovered at 84 GHz as a strong maser by Batrla and Menten (1988) in DR21(OH). The next transition is  $6_{-1} - 5_0 E$ , at 133 GHz. The methanol line in this transition was first observed by Cummins et al. (1986) from Sgr B2, but it was not clear if it was a maser line. In this paper, we report on the detection of the maser emission from many sources in the transition  $6_{-1} - 5_0 E$  at 133 GHz.

## 2. Observations

The observations were made on June 5 — 7, 1995 with the 12-m NRAO<sup>1</sup> telescope at Kitt Peak. For the first time, the observations were conducted in remote observing mode from the Astro Space Center in Moscow. For this purpose, a Sun workstation at the Astro Space Center was connected via Internet to the computer of the 12-m telescope. An astronomer in Moscow could see on the screen of his computer the status of the telescope, the weather information, and a TV monitor of the telescope inside the dome and environs, and was also able to converse with the telescope operator using the ‘talk’ procedure. The spectra were monitored in real time using the UNIPOPS software package. The communication between the telescope and Astro Space Center was rather stable, with only one short break during the 48-hour observing session. The observations of the methanol line were carried out at the rest frequency of the  $6_{-1} - 5_0$   $E$  transition, 132890.790 MHz (Lees et al. 1973), with the dual-polarization SIS receiver. Two other methanol lines were also observed near this frequency:  $5_{-2} - 6_{-1}$   $E$  at 133606.5 MHz and  $6_2 - 7_1$   $A^-$  at 132621.94 MHz. The typical system noise temperature was 200 to 250 K. The observations were performed in position-switching mode. The beamwidth was 41", and the pointing accuracy was better than 5". The calibration was achieved by the standard vane method, and for a point source, 1 K of  $T_R^*$  was equal to 35 Jy. A hybrid spectrometer with 37.5 MHz total bandwidth and 384 channels in each polarization was used, providing velocity resolution of 0.11 km s<sup>-1</sup>.

---

<sup>1</sup>NRAO is operated by Associated Universities, Inc., under contract with the National Science Foundation.

### 3. Results

Forty-one sources were observed with a detection limit of 1.75 Jy. The list of sources included known methanol masers both of Class I and Class II. The emission line of methanol was detected from 35 sources, the non-detections being Class II methanol masers associated with IRAS sources. In the rest of the Class II methanol masers, thermal emission was detected. On the contrary, many of the Class I masers showed intense narrow, evidently maser lines at 133 GHz. We tentatively define as masers sources which show narrow lines with line width less than  $1 \text{ km s}^{-1}$ . An additional evidence of the maser emission would be its high brightness temperature, exceeding, e.g.  $10^4 \text{ K}$ . Unfortunately, present observations were made with a low angular resolution provided by the  $41''$  beam of the 12-m Kitt Peak telescope. If one assumes that the sources were unresolved by the telescope beam with the upper limit of the angular size of  $20''$ , then the lower limit of the brightness temperature even for the stronger sources DR21(OH) and DR21-W is only 150 K. Observations with a much higher angular resolution at millimeter interferometers such as the BIMA array or Plateau de Bure interferometer are needed in order to firmly establish the maser nature of the emission lines. Here we report on new maser sources defined as above. Their spectra are shown in Fig.1, and the Gaussian line parameters are given in Table 1. Results on the rest of the sources will be reported elsewhere. In the transitions  $5_{-2} - 6_{-1} E$  and  $6_2 - 7_1 A^-$ , predicted by Cragg et al. (1992) as Class II methanol masers, no lines were detected in the new maser sources except for weak wide lines in DR21(OH).

#### 3.1. Notes on individual sources

**OMC – 2.** The  $6_{-1} - 5_0 E$  spectrum (Fig.1) can be approximated by a strong, narrow, most probably maser line, and a weak broad pedestal line. The narrow line is at the same

radial velocity as maser lines in the  $7_0 - 6_1 A^+$  transition at 44 GHz and the  $4_{-1} - 3_0 E$  transition at 36 GHz (Haschick, Menten, and Baan 1990), the  $5_{-1} - 4_0 E$  transition at 84.5 GHz (Menten 1991), the  $5_2 - 5_1 E$  and  $6_2 - 6_1 E$  transitions at 25 GHz (Menten et al. 1988b), and the  $8_0 - 7_1 A^+$  transition at 95 GHz (Menten 1991, Val'tts et al. 1995). The line width is somewhat larger ( $0.68 \text{ km s}^{-1}$ ) at this frequency than at 44 GHz ( $0.35 \text{ km s}^{-1}$ ), where flux density is the highest. The broad component was not seen in these transitions but was observed by Menten et al. (1988a) in  $2_k - 1_k$  thermal lines of methanol at 96 GHz.

**NGC2264.** The  $6_{-1} - 5_0 E$  spectrum (Fig.1) also shows a superposition of a narrow maser line and a broad line at close radial velocities. A similar two-component spectrum was observed in the  $4_{-1} - 3_0 E$  transition at 36 GHz (Haschick, Menten, and Baan 1990), the  $5_{-1} - 4_0 E$  transition at 84.5 GHz (Menten 1991), and the  $8_0 - 7_1 A^+$  transition at 95 GHz (Val'tts et al. 1995). In the transition  $7_0 - 6_1 A^+$  at 44 GHz there are two narrow lines separated by  $0.28 \text{ km s}^{-1}$  (Haschick, Menten, and Baan 1990). At 132 GHz the line is broader,  $0.84 \text{ km s}^{-1}$ , and may be a blend of two narrow lines. See also the collection of spectra at frequencies from 36 to 146 GHz of Menten (1991). Menten also shows a broad absorption profile at 12.1 GHz ( $2_0 - 3_{-1} E$ ) with width and shape similar to the broad emission at 36 GHz.

**M8E.** This methanol maser was first detected at 36 GHz (Kalenskii et al. 1994), then found to be one of the most powerful masers at 44 GHz (Slysh et al. 1994). At 133 GHz, it is not so strong, with a flux density of about 60 Jy; the profile is something broader and consists of an intense narrow component and a weak, broad component (Fig.1).

**W33 – Met.** This source has a narrow maser line at a radial velocity of  $32.8 \text{ km s}^{-1}$  and a broad line shifted by  $4 \text{ km s}^{-1}$  to higher velocities (Fig.1). At other methanol transition frequencies, there is a narrow maser line at 9.9 GHz in the transition  $9_{-2} - 8_{-1} E$  (Slysh et al. 1992); at 25 GHz, the maser lines are seen at the radial velocity  $33.2 \text{ km s}^{-1}$  in the transitions  $J_2 - J_1 E$  with  $J=3$  to 6, and 9, at the radial velocity  $36.3 \text{ km s}^{-1}$ , there is a broad

line in transitions  $J=2$  to 6 (Menten et al. 1986). At 36 GHz ( $4_{-1} - 3_0 E$ ), the spectrum is similar, with the narrow maser line and broad line red shifted by  $4.2 \text{ km s}^{-1}$  (Kalenskii et al. 1994). Similar two-component spectra were observed at 44 GHz ( $7_0 - 6_1 A^+$ ) by Haschick, Menten and Baan (1990) and at 95 GHz ( $8_0 - 7_1 A^+$ ) by Val'tts et al. (1995). Pratap and Menten (1993) mapped the 95 GHz maser and found that its position coincides with the position of the 25 GHz maser to within about  $2''$ .

**L379.** The  $6_{-1} - 5_0 E$  spectrum (Fig.2, left middle spectrum) shows a double-peaked line with intense wings. The line has been separated into four Gaussian components, with two narrow, probably maser lines, with  $0.8$  and  $1.2 \text{ km s}^{-1}$  line width (Table 1). The methanol maser in L379 was first discovered at 44 GHz and 36 GHz (Kalenskii et al. 1992). The shape of the line at 36 GHz with two peaks is similar to the shape at 133 GHz. A moderately strong line was found at 95 GHz (Val'tts et al. 1995) with line width  $3.9 \text{ km s}^{-1}$ . This rather large line width probably results from a blend of several narrow maser lines. Other evidence of the maser nature of the 133 GHz emission comes from a comparison of the intensity of this line with the two other methanol lines observed in this experiment. In Fig.2 (left) spectra of the three methanol transitions near 133 GHz are presented in comparison with a similar set of spectra of Ori-KL (Fig.2, right). While in Ori-KL the lines are present in all three transitions with relative intensities proportional to the line strength that is typical for the thermal emission, in L379 only the  $6_{-1} - 5_0 E$  line is present, and the two other lines are weaker than 0.03 of this line. This is consistent with a non-thermal distribution of line intensities and maser amplification in the  $6_{-1} - 5_0 E$  line. Several sources also show only the  $6_{-1} - 5_0 E$  line with a moderately narrow line width, and are probably relatively weak masers: NGC2071, S255, S231, GGD27. They are Class I methanol masers in other transitions.

**DR21(OH) and DR21 – W.** These two strongest 133 GHz masers separated by  $3'.6$  show very intense narrow maser lines superposed on a broad component (Fig.1). The narrow

maser line in DR21(OH) was observed in other methanol transitions at 36, 44, 84, 95 GHz, and in DR21–W at 25, 36, 44, 84, 95 GHz (Menten et al. 1986, Haschick et al. 1990, Batrla and Menten 1988, Plambeck and Menten 1990, Menten 1991) at the same radial velocity. The broad line was observed in DR21(OH) at 25, 36, 44, 84 and 95 GHz, and in DR21–W only at 95 GHz. In DR21(OH) broad lines in  $5_{-2} - 6_{-1}$   $E$  and  $6_2 - 7_1$   $A^-$  transitions were found at the same radial velocity as the broad component in  $6_{-1} - 5_0$   $E$  transition, with the intensity of about 5 per cent of the  $6_{-1} - 5_0$   $E$  line intensity.

#### 4. Discussion

The similarity between line profiles of the new 133 GHz methanol masers and methanol masers of Class I as well as association with the same sources, suggests that the 133 GHz methanol masers belong to the Class I. The corresponding methanol transition  $6_{-1} - 5_0$   $E$  is of the same type  $K = -1 \rightarrow K = 0$ , as most of the Class I transitions in methanol– $E$ . The detection of new masers in the transition  $6_{-1} - 5_0$   $E$  supports the suggestion that  $K = -1$  ladder levels are overpopulated relative to  $K = 0$  ladder levels, which is the cause for the inversion of  $J_{-1} - (J - 1)_0$  transitions. A natural way of overpopulating the  $K = -1$  ladder is collisional excitation followed by spontaneous decay. The decay rates are different for the two ladders: for the upper  $6_{-1}$  level the spontaneous decay rate is  $1.07 \times 10^{-4} \text{ s}^{-1}$ , while for the lower  $5_0$  level it is a factor of two higher  $2.12 \times 10^{-4} \text{ s}^{-1}$ . The molecules excited by collisions to the  $6_{-1}$  level remain there longer than at the  $5_0$  level, resulting in the higher population of the  $6_{-1}$  level. The higher population of the upper level in the  $6_{-1} - 5_0$   $E$  transition, or population inversion (relative to the normally lower population of the upper level in thermally excited molecules) may produce the maser emission if the column density is high enough to provide significant amplification. The same mechanism of level population inversion holds for other similar transitions in methanol– $E$ :  $4_{-1} - 3_0$ ,  $5_{-1} - 4_0$ ,  $7_{-1} - 6_0$ ,



$8_{-1} - 7_0$ , and so on. In methanol-A, the  $7_0 - 6_1$ ,  $8_0 - 7_1$ ,  $9_0 - 8_1$  etc. transitions can be inverted in the same manner. A comparison of 133 GHz masers with the strongest Class I methanol masers at 44 GHz shows that both show emission features at the same radial velocities. One can suppose that the emission features at both frequencies originate from the same region. Compared to the 44 GHz masers, the 133 GHz masers are weaker: the flux density is a factor of 5 to 27 lower, and the line width is a factor of 1.4 to 4 larger. The flux density ratio is roughly consistent with the calculated optical depth ratio of about 6; this is expected for saturated masers at both frequencies. On the other hand, the observed larger line width at 133 GHz as compared to 44 GHz is more appropriate for unsaturated masers, where the line width is inversely proportional to the square root of the optical depth. This apparent contradiction can be resolved if the masers are saturated but the line rebroadening due to the saturation does not take place, because the velocity distribution undergoes cross relaxation toward a Maxwellian distribution as a result of elastic collisions (Nedoluha and Watson 1988). Therefore, line narrowing can be expected in the saturated masers, also; in the case of Class I methanol masers, collisions are important both for the maser pump and for the velocity distribution relaxation, which permits line narrowing.

## 5. Summary

The first successful remote observations from Moscow with the NRAO Kitt Peak radio telescope have resulted in the detection of new Class I methanol masers at 133 GHz. The millimeter-wave masers are as widespread as the longer-wavelength masers: 35 sources were detected in emission; at least seven are definite masers, and several more are good candidates. Two other methanol lines were used to discriminate between maser and thermal emission. The properties of the new maser sources are better described by the saturated maser model, although the line width arguments require cross relaxation to explain the lack

of line rebroadening.

We are grateful to Dr. Phil Jewell, Dr. K. Mead and the staff of the NRAO Kitt Peak radio telescope for help with the observations. The Sun Sparc station used in the remote observations was made available to the Astro Space Center through a grant from the National Science Foundation to the Haystack Observatory. This work was supported by the Russian Foundation for Basic Research (grant 95–02–05826).

Fig. 1.— Spectra of the newly detected 133 GHz methanol- $E$  masers.

Fig. 2.— 133 GHz methanol spectra in three transitions for L379 (left) and Ori KL (right). Note the anomalously large relative strength of the  $6_{-1}-5_0$   $E$  maser line in L379 as compared to the apparently thermal line ratio in Ori KL.

## REFERENCES

- Batrla, W., & Menten, K.M., 1988, *ApJ*, 329, L117
- Cragg, D.M., Johns, K.P., Godfrey, P.D., & Brown, R.D., 1992, *MNRAS*, 259, 203
- Cummins, Sally, E., Linke, R.A., & Thaddeus, P., 1986, *ApJS*, 60, 819
- Haschick, A.D., & Baan, W.A., 1989, *ApJ*, 339, 949
- Haschick, A.D., Menten, K.M., & Baan, W.A., 1990, *ApJ*, 354, 556
- Kalenskii, S.V., Bachiller, R., Berulis, I.I., Val'tts, I.E., Gomez-Gonzalez, J., Martin-Pintado, J., Rodriguez-Franco, A., & Slysh, V.I., 1992, *Astron.Zh.*, 69, 51
- Kalenskii, S.V., Berulis, I.J., Val'tts, I.E., Dzura, A.M., Slysh, V.I., & Vasil'kov, V.I., 1994, *Astron.Zh.*, 71, 51
- Lees, R.M., Lovas, F.J., Kirchhoff, W.H., & Johnson, D.R., 1973, *J. Chem. Ref. Data*, 2, 205
- Menten, K.M., 1991, in "Skylines", Proceedings of the Third Haystack Observatory Meeting, ed. Haschick, A.D., & Ho, P.T.P., San Francisco: Astronomical Society of the Pacific
- Menten, K.M., Walmsley, C.M., Henkel, C., & Wilson, T.L., 1986, *A&A*, 157, 318
- Menten, K.M., Walmsley, C.M., Henkel, C., & Wilson, T.L., 1988a, *A&A*, 198, 253
- Menten, K.M., Walmsley, C.M., Henkel, C., & Wilson, T.L., 1988b, *A&A*, 198, 267
- Morimoto, M., Ohishi, M., & Kanzawa, T., 1985, *ApJ*, 288, L11
- Nedoluha, G.E., & Watson, W.D., 1988, *ApJ*, 335, L19
- Plambeck, R.L., & Menten, K.M., 1990, *ApJ*, 364, 555
- Pratap, P., & Menten, K., 1993, in "Astrophysical Masers", eds Clegg, A.W., & Nedoluha, G.E., Lecture Notes in Physics, Springer-Verlag

Slysh, V.I., Kalenskii, S.V., & Val'tts, I.E., 1992, ApJ, 397, L43

Slysh, V.I., Kalenskii, S.V., & Val'tts, I.E., 1994, MNRAS, 268, 464

Slysh, V.I., Kalenskii, S.V., & Val'tts, I.E., 1995, ApJ, 442, 668

Val'tts, I.E., Dzura, A.M., Kalenskii, S.V., Slysh, V.I., Booth, R., & Winnberg, A., 1995,  
A&A, 294, 825

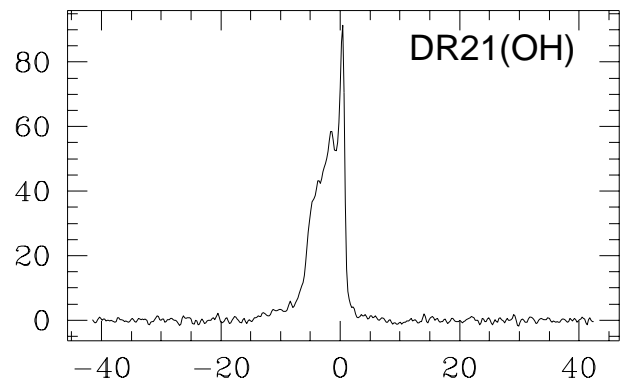
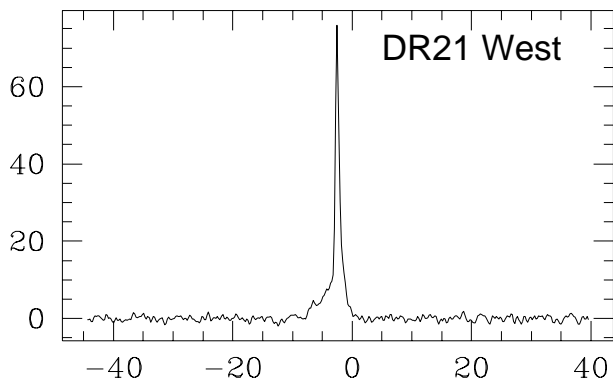
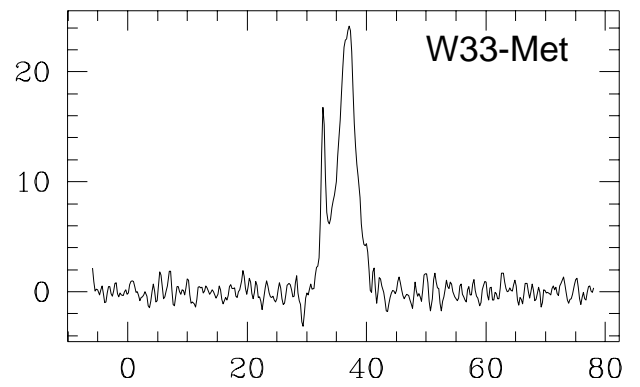
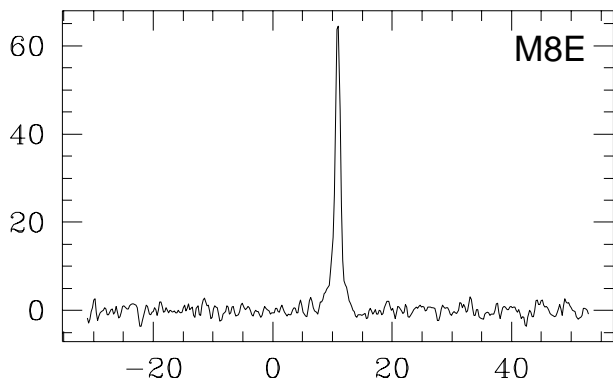
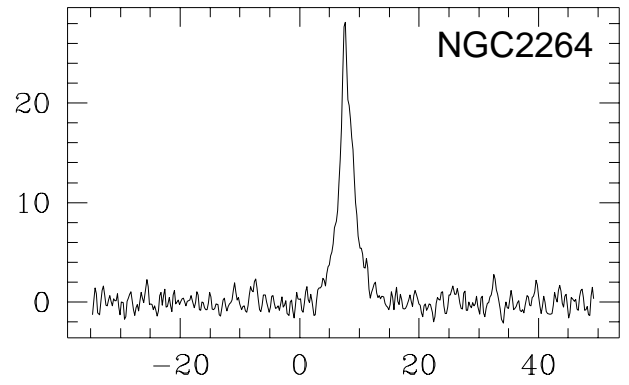
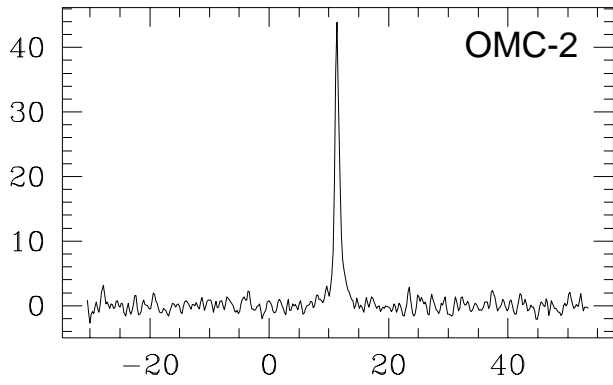
Zuckerman, B., Turner, B.E., Johnson, D.R., Palmer, P., & Morris, M., 1972, ApJ, 177, 601

Table 1. Line Parameters Determined from  $6_{-1} - 5_0$   $E$  Observations

Name	R.A.(1950)	Dec.(1950)	S(Jy)	$V_{lsr}$ (km s $^{-1}$ )	$\Delta V$ (km s $^{-1}$ )
OMC-2	05 32 59.8	-05 11 29	36.8(1.0)	11.39(0.01)	0.68(0.02)
	...	...	7.8(0.1)	11.66(0.07)	2.50(0.19)
NGC2264	06 38 24.9	09 32 28	11.3(0.8)	7.54(0.02)	0.84(0.07)
	...	...	17.4(0.6)	7.94(0.04)	3.77(0.10)
M8E	18 01 49.7	-24 26 56	12.9(1.2)	10.61(0.06)	2.68(0.16)
	...	...	55.2(1.3)	10.92(0.01)	0.77(0.02)
W33-Met	18 11 15.7	-17 56 53	15.0(0.6)	32.78(0.02)	1.02(0.05)
	...	...	23.3(0.3)	36.76(0.02)	3.57(0.06)
L379	18 26 32.9	-15 17 51	11.6(0.5)	16.39(0.15)	12.63(0.26)
	...	...	10.5(0.6)	17.69(0.02)	0.80(0.06)
	...	...	40.9(0.7)	18.96(0.03)	4.81(0.06)
	...	...	18.8(0.6)	20.24(0.02)	1.20(0.05)
DR21-W	20 37 07.6	42 08 46	11.3(0.5)	-2.76(0.06)	4.20(0.15)
	...	...	64.7(0.8)	-2.47(0.01)	0.62(0.01)
DR21(OH)	20 37 13.8	42 12 13	63.4(1.6)	0.28(0.01)	0.86(0.02)
	...	...	56.7(0.6)	-2.34(0.04)	5.65(0.08)

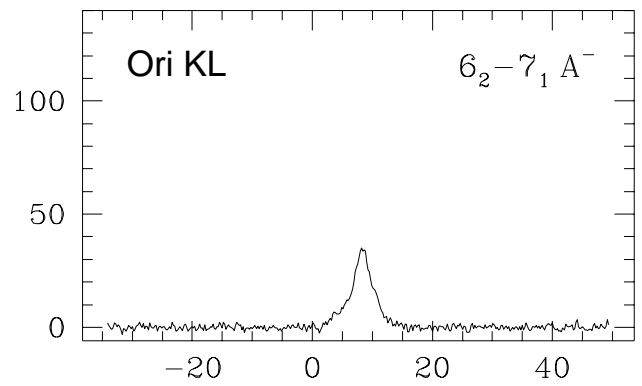
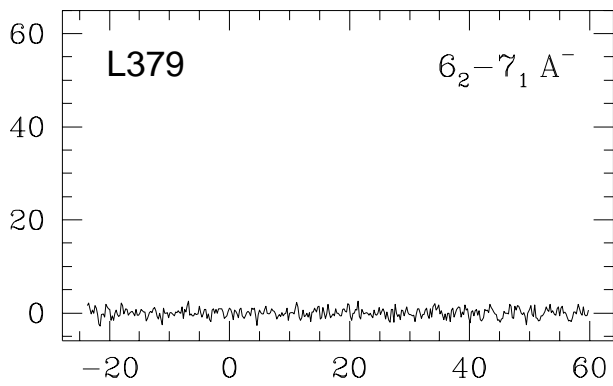
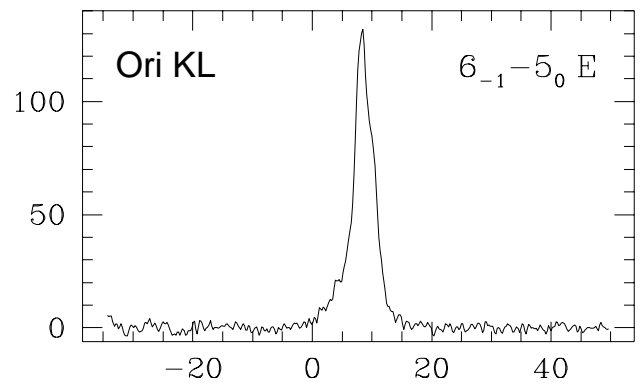
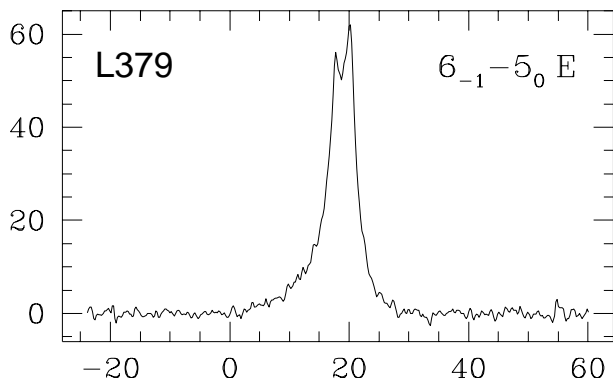
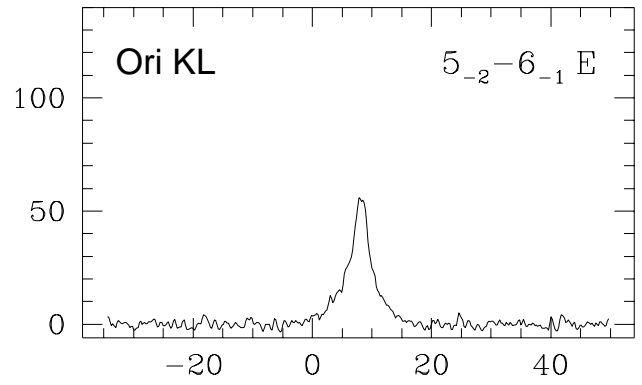
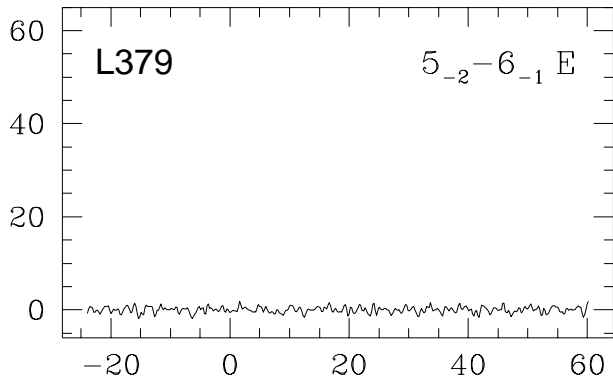
Notes: Errors are  $1 \sigma$  deviations determined from Gaussian fits.

FLUX DENSITY (Jy)



LSR VELOCITY ( $\text{km s}^{-1}$ )

FLUX DENSITY (Jy)



LSR VELOCITY ( $\text{km s}^{-1}$ )